ULTRALOW PERCOLATION THRESHOLD IN POLYAMIDE 6.6 / MWCNT COMPOSITES

Beate Krause, Regine Boldt, Liane Häußler, Petra Pötschke*

Leibniz Institute of Polymer Research Dresden, Hohe Str. 6, 01069 Dresden, Germany

**Corresponding author: Tel. +49 351 4658 395, Fax +49 351 4658 565. E-mail address:poe@ipfdd.de (P. Pötschke)*

Abstract

When incorporating of multiwalled carbon nanotubes (MWCNTs) synthesized by the aerosol-CVD method using different solvents into polyamide 6.6 (PA66) by melt mixing an ultralow electrical percolation threshold of 0.04 wt.% was found. This very low threshold was assigned to the specific characteristic of the MWCNTs for which a very high aspect ratio, a good dispersability in aqueous surfactant dispersions, and relatively low oxygen content near the surface were measured. The investigation of the composites by transmission electron microscopy on ultrathin cuts as well as by scanning electron microscopy combined with charge contrast imaging on compression moulded plates illustrated a good MWCNT dispersion within the PA66 matrix and that the very high aspect ratio of the nanotubes remained even after melt processing. Additionally, the thermal behaviour of the PA66 composites was investigated using differential scanning calorimetry (DSC) showing that the addition of only 0.05 wt.% MWCNT leads to an increase of the onset crystallization temperature of 11 K.

Keywords

A. Carbon nanotubes, Polymer-matrix composites (PMCs), **B.** Thermal properties, **D.** Differential scanning calorimetry (DSC), Scanning/transmission electron microscopy (STEM)

1. Introduction

Carbon nanotube (CNT) based polymer composites have a very high potential in different industrial applications. Their property profile depends as well on CNT properties, dispersion and orientation aspects, interfacial adhesion and matrix properties which can widely vary. The CNT properties like nanotube length, diameter, bulk density, and waviness are dependent on the CNT synthesis method used and the synthesis conditions [1]. CNT purity, functional groups on the surface of the CNTs, their entanglements and strength of agglomerates influence the dispersability of CNT in different media like solvents or polymers [2, 3]. For the effective use of carbon nanotubes excellent dispersion and distribution within the hosting matrix are essential, even if some secondary agglomeration may help to establish the electrically conductive networks needed for electrical conductivity [4]. Additionally, the aspect ratio of nanotubes significantly affects the achievable electrical percolation threshold [5] and mechanical properties of the composites [6-8]. If the aspect ratio becomes lower, the formation of a percolated conductive network requires a higher CNT content [9, 10]. The aspect ratio of CNTs is controlled by the synthesis condition and the fact that nanotubes break during processing, e.g. ball milling, ultrasound and melt compounding [3, 6, 11-19].

In the literature only few papers discuss melt mixed polyamide 6.6 (PA66)/CNT composites. Krause et al. [1] studied the electrical percolation using small-scale melt

mixing on compression moulded plates of PA66 containing five different kinds of CNTs resulting in percolation thresholds between 0.04 and 1.02 wt.%. The lowest percolation thresholds of 0.041 wt.% and 0.048 wt.% were found for nanotubes synthesized via aerosol-catalytically vapour deposition technique using the solvents acetonitrile (MWCNT 1) or cyclohexane (MWCNT 2), respectively (see Figure 1). This exceptional low, called 'ultralow', percolation threshold of aerosol CNTs was assigned to some of the properties of these CNTs [1]. XPS measurements showed for MWCNT 1 the incorporation of 5.57 wt.% nitrogen in the CNT surface composition and the formation of a bamboo-like structure as visualised by transmission electron microscopy (TEM). The number of carbon shells varied between 4 and 10 and the outer diameter between 8 and 40 nm. For the CNT synthesized with cyclohexane (MWCNT 2) a tubular CNT structure with up to 50 carbon shells and an outer diameter of 10 – 80 nm was found using TEM. For both kinds of CNTs low oxygen contents of 0.76 wt.% (MWCNT 1) or 1.06 wt.% (MWCNT 2) were determined by XPS. Scanning electron microscopy (SEM) images of the cryofractured PA66 composites containing MWCNT 1 and MWCNT 2 showed well dispersed nanotubes that are relatively long up to a length of 2 µm. Quantification of the macrodispersion of these both MWCNTs using transmission light microscopy (LM) on thin sections of the composites resulted in an agglomerate area ratio of 2.0 area%. Mean agglomerate diameters of 17 ± 2 µm (MWCNT 1) and 8 ± 3 µm (MWCNT 2) were found. Furthermore, the dispersability in aqueous surfactant solution of both synthesized nanotubes (in [20] CNT3 (cyclohexane) and CNT4 (acetonitrile)) and Nanocyl™ NC7000 were investigated with centrifugal separation analysis using an analytical centrifuge LUMiFuge® [20]. After 30 min ultrasonic treatment to disperse the CNTs in the aqueous surfactant solution all three

CNT dispersions were stable during 45 min centrifugation indicating a high dispersability. This high dispersability correlates with the low electrical percolation thresholds in polyamide 66 composites as compared to the other CNTs used in this study. Using the same preparation conditions as well as the same PA 66, for Nanocyl^{TM} NC7000 an electrical percolation threshold of 0.18 wt.% was found [20], which is much higher than that obtained for MWCNT1 and MWCNT2 in [1] (see Figure 1).

Caamaño et al. [21] reported electrical percolation thresholds between 1.48 and 2.25 wt.% for melt mixed PA66 composites filled with different MWCNTs produced by Southwest Nanotechnologies (SWeNT, US) which differ in diameter, length and structure while a comparable microcompounder but different mixing conditions as compared to the study in [1] were used. Furthermore, an increase of crystallization temperature of about 10 K independent on the CNT content was found in that study, whereas the melting temperature was not influenced by the incorporation of CNTs. Results of the thermal behaviour with the same tendency were also described for PA66/MWCNT fibres by Baji et al. [22], for PA66/MWCNT composites containing nanotubes with different kind of functionalization by Oui et al. [23], and for melt mixed polyamide/MWCNT composites by Krause et al. [24].

Investigations of the carbon nanotube dispersion in PA66 composites using scanning electron microscopy and transmission light microscopy were reported by the authors of the present study [1, 20, 24] showing that a good CNT dispersion is difficult to achieve in PA66 composites as indicated by nanotube agglomerates in macro and nano scale. Furthermore, Villmow et al. [25] found for poly(lacid acid) (PLA) composites containing 7.5 wt.% MWCNT an influence of the CNT dispersion quality on the degree of crystallinity. The crystallinity of the PLA matrix was as higher as better the nanotube

dispersion. A relation between the crystallinity and the electrical percolation threshold of polyethylene and polypropylene-ethylene copolymers filled with singlewalled CNTs was described by Jeon et al. [26]. It was found that the electrical percolation threshold decreased with increasing crystallinity of the polymer, whereas the most significant changes in percolation behaviour occur at crystallinity contents below 35%. At higher degree of crystallinity only negligible differences between the percolation thresholds could be observed.

The aim of the present investigation is to study deeper and find an explanation for the ultralow electrical percolation threshold (0.04-0.05 wt.%) of PA 66 composites containing the two samples of MWCNTs synthesized by the aerosol method [1]. To our knowledge, this is the lowest threshold reported for melt mixed PA66 composites, but also for other melt mixed polymer-CNT systems [27]. For this purpose, next to the findings already published in [1,17], especially the morphology of the composites at nano and macro scale were studied. In addition, changes in the crystallization behaviour were investigated motivated by findings, that there is an interrelation between nanotube dispersion quality and crystallinity [25] as well as crystallinity and percolation threshold [26]. For comparison PA66 composites filled with the commercial available MWCNTs Nanocyl^{TM} NC7000 were prepared.

2. Experimental

Powder of polyamide 6.6 (PA66, VYDYNE, Solutia Inc., Belgium) with a melt flow index of 600 g/10 min (275 °C, 5 kg, ASTM Test Method D1238) was melt mixed with MWCNTs synthesized at the Leibniz Institute for Solid State and Materials Research Dresden via aerosol-catalytically vapour deposition technique using the solvents

acetonitrile (MWCNT 1, bamboo-like structure) or cyclohexane (MWCNT 2, tubular structure) [1].

The melt compounding of the PA66/MWCNT composites was performed using DACA microcompounder (DACA Instruments, Goleta, USA) at 280 °C with a rotation speed of 50 rpm for 5 min and is described in detail in [24]. After processing strands of about 2 mm diameter were let out using the set speed to air without additional cooling. For the measurement of the electrical properties the composites were compression molded at 320°C [24].

For transmission light microscopy (LM) characterization samples were cut from the extruded strands into thin sections with a thickness of 10 µm using a microtome Leica 2055 (Leica Mikrosysteme Vertrieb GmbH, Bensheim, Germany) and were fixed with Entellan® (Merck KGaA, Darmstadt, Germany) on glass slides. The LM investigations were performed using a microscope BH2 combined with a camera DP71 (Olympus Deutschland GmbH, Hamburg, Germany).

TEM images were recorded using a Zeiss Libra200MS (Carl Zeiss GmbH, Germany, field emission cathode, point resolution 0.2 nm) with an acceleration voltage of 200 kV. Ultrathin sections of 60 nm thickness were cut from extruded strands at -60 °C using a Leica Ultracut UC6 cryomicrotome (Leica, Austria) in combination with a diamond knife (35° cut angle; Diatome, Switzerland).

Morphological characterization of the MWCNTs and the composites was performed using scanning electron microscopy (SEM) (Ultra plus microscope, Carl Zeiss GmbH, Germany, field emission cathode). The MWCNT materials were investigated as received dry powders. SEM observation of the composite materials was performed on the compression moulded plates using an InLens detector by monitoring the charge

contrast imaging (CCI) visualizing the electrical conductive filler network of the samples [28]. Additionally, the composite strands were cryo-fractured in liquid nitrogen and the surfaces were studied after platinum sputtering.

Differential scanning calorimetry (DSC) was performed using a Q1000 (TA-Instruments, New Castle, USA) in the temperature range of –60 °C to 300 °C at a scan rate of ±10 K/min. Samples of about 5 mg were investigated under nitrogen atmosphere in a heating-cooling-heating cycle. The melting temperature T_m and the melting enthalpy ΔH_m were calculated from the 2nd heating run. For the calculation of the crystallinity α the value of melting enthalpy of 100 % crystalline PA66 (190 J/g) was used [29].

The electrical resistivity of a compact package of the pure CNT powders was measured using PuLeMe (**Pu**lver**le**itfähigkeits**me**ssung) instrument, developed and constructed at the Leibniz Institute of Polymer Research Dresden. The PuLeMe device was set up in order to measure the electrical conductivity of powdery substances. The powder to be examined (40-50 mg) is filled into a cylinder (40 mm length, 5 mm diameter) and compressed by a piston up to a pressure of 30 MPa using a stepper motor. During the compression process, the electric resistance is continuously measured between two gold electrodes located on top of the piston and on the bottom of the cylinder using a Keithley 2001 electrometer. The conductivity derived from the resistance and the geometry data is then recorded against the pressure. The control of the device as well as the data acquisition and analysis is carried out by custom-made software developed with TestPoint^{TM}. The software allows user programming of different cycles and automatic control. In addition, the density of the material at 30 MPa was calculated from the mass

of CNTs and the final thickness of the different compacted nanotube cylinders, which varied between 2.2 and 3.6 mm.

3. Results

3.1. Morphological study of the MWCNTs

Firstly, next to morphology studies of single nanotubes by TEM (reported in Ref. [1], Fig. 4) the morphology of the dry nanotube powders was observed using SEM and TEM (Figure 2). For both types of aerosol-synthesized nanotubes (MWCNT 1, MWCNT 2) a stretched and aligned shape was found, similar to the growth of nanotube forests. Figure 2 c illustrates the bamboo-like structure of MWCNT 1. The length of the CNTs was estimated to be in the range between 50 and 100 µm. In contrast, the Nanocyl^{TM} NC7000 are synthesized as spherical agglomerates with an inner combed yarn like structure (see Figure 2 d, e). The nanotubes are characterized by a tubular structure (Fig. 2 f) and an entangled shape. The mean nanotube length of the as-grown Nanocyl^{TM} NC7000 was measured to be 1.3 µm [3]. The comparison of the aerosol-synthesized nanotubes and the Nanocyl^{TM} NC7000 shows that the aspect ratio of the aerosol-synthesized MWCNT 1 and 2 is about 100 times larger. This higher aspect ratio contributes to the much lower electrical percolation threshold of MWCNT 1 and 2.

3.2 MWCNT powder conductivity

Based on the expectation that the electrical conductivity of the nanotubes itself may influence electrical composite properties, the electrical conductivity of pure CNT powders was measured. The values ranged between 4 and 30 S/cm (at a pressure of 30 MPa). The nanotubes synthesized with cyclohexane (MWCNT 2) showed a low value

of 4 S/cm, whereas for the nanotubes synthesized with acetonitrile (MWCNT 1) a higher conductivity of 30 S/cm was determined. The compacted samples exhibited different densities depending on the kind of CNTs. The densities of compacted CNTs at 30 MPa were determined to be 1.33 g/cm^3 (MWCNT 1) and 2.36 g/cm^3 (MWCNT 2) indicating different compressibilities of the nanotube powder materials. In comparison to these results, CNT conductivities of 15 S/cm and 24 S/cm and densities of 0.95 g/cm^3 and 1.04 g/cm^3 were found for the compacts of the commercial carbon nanotubes Nanocyl^{TM} NC7000 and Baytubes® C150P, respectively. Thus, the conductivity of CNT powders obviously does not directly correlate with the electrical properties of the composites.

3.3 Morphology of composites

To characterize the macrodispersion of MWCNTs in the PA66 matrix at low filling grades near the electrical percolation threshold light microscopy analysis on thin sections was performed. Some agglomerates were found in the composites even at the very low CNT concentration of 0.05 wt.% (Figure 3). Although a higher number of remaining agglomerates in the PA66/MWCNT1 composite was found in comparison to the PA66/NC7000 composite, at 0.05 wt.% a conductive network was formed only in the PA66/MWCNT1 composite as indicated by a volume conductivity of $7*10^{-5}$ S/cm. As already found in many studies [4, 24, 30, 31], the CNT macrodispersion in a composite obviously also does not correlate directly with the electrical properties of the composites, even if it gives an impression how much of the incorporated nanotube material is still present in agglomerates and not dispersed as individual tubes which mainly determine the conductive network.

To study the specific of the conductive network in more detail, the nanoscale dispersion of the CNTs in the polyamide matrix was characterized using TEM investigations on ultrathin cuts. Figure 4 a shows well-dispersed nanotubes for the composite with 0.05 wt.% MWCNT 1. As a consequence of the very low CNT concentration and a part of the CNTs being embedded in the macro agglomerates as observed by light microscopy, the number of evaluated nanotubes was very low. However, the visible nanotubes are characterized by a remarkable stretched shape and very high lengths even after the melt processing (Figure 4 b). In Figure 4 c a TEM image of PA66/0.05 wt.% NC7000 is presented. In contrast to the PA66/MWCNT1 composite, the CNT dispersion is incomplete and the distribution inhomogeneous and only a few entangled nanotubes in clusters could be observed. In addition, the length of the visible nanotubes is much lower.

In addition, the morphology of the conductive network inside the composites was investigated using SEM in the charge contrast imaging mode (CCI). In this method, only the nanotubes contributing to the conductive network are visible as white spots. Figure 5 a and b show a segregated network structure within the PA66/MWCNT1 composite. Obviously, several conductive pathways spanning the sample result in the ultralow electrical percolation threshold. In addition, these images also show the stretched shape of the nanotubes, as it was seen before in the TEM images. An estimation of the nanotubes length from SEM-CCI images leads to values up to about 3-7 µm. These are very high lengths considering that the nanotubes were melt processed which was found to lead to a significantly nanotube shortening [3, 12-14]. For a detailed measurement of the CNT length after processing dissolving the CNTs from the matrix would be necessary, which was not performed within this study. For comparison the

PA66/ 1wt.% NC7000 composite was investigated. Only few short and entangled nanotubes are visible embedded in a CNT free region appearing black in the image (Figure 5 c). Comparing the PA66 composites containing 1 wt.% (Figure 5 b and c) the conductive network in PA66/MWCNT1 composite appears significantly more homogeneous and denser packed than the PA66/NC7000 composite.

The long and stretched shape of the bamboo-like nanotubes was also observed on the surface of cryofractured composites containing 0.05 wt.% MWCNT 1 (Figure 6 a). Some CNTs were visible as white dots if only one end of the nanotubes was on the surface of the fracture. Other CNTs were sticking out and were visible on the surface showing lengths up to about 1 µm. In contrast, for the composite containing Nanocyl^{TM} NC7000 no nanotubes were visible at the surface (Figure 6 b).

3.4. Discussion of reasons for ultralow percolation

In order to explain the found ultralow electrical percolation threshold of 0.04-0.05 wt.% of the aerosol-synthesized nanotubes within PA66, the combination of several favorable factors can be assumed. These are the high nanotubes length, the stretched nanotube shape and the relatively good nanotubes dispersion resulting in the formation of conductive pathways already at such low loadings. Thereby, the structural CNT parameters may support the good dispersion which was found in aqueous solution [20] and the PA66 matrix and the easy formation of the conductive network. In contrast, the NC7000 nanotubes are significantly shorter and entangled. In addition, the high surface purity of aerosol-synthesized MWCNTs as shown in [1] using XPS by low oxygen contents may contribute to low contact resistances at the touching points or between neighboured nanotubes and may donate to higher conductivity values of the formed

nanotube network. Interestingly, the electrical conductivity of the CNT powders (MWCNT 1 and 2, NC7000, Baytubes® C150P) measured under pressure do not correlated with the electrical properties of the PA66 composites. The nitrogen content within MWCNT 1 may be assumed to be favourable for good dispersion within the PA66 matrix, however similar good dispersion and low percolation threshold were also achieved with MWCNT 2 not having nitrogen in its structure.

3.5 Thermal behaviour

The thermal behaviour of the filled PA66 composites was investigated using DSC in order to study the effect of MWCNTs on matrix crystallization and to proof if differences in nanotube dispersion are reflected in the thermal properties, especially crystallinity. It was found that the crystallization temperature increases with the addition of CNTs. This nucleating effect of CNTs is known and has been described by various authors [21-23, 32, 33]. For both aerosol-synthesized MWCNTs the incorporation of 0.05 wt.% MWCNTs caused an increase in the onset crystallization temperature $T_{c,o}$ of 11 K and an increase in the maximum crystallization temperature $T_{c,m}$ of 7 K in comparison to the comparably processed PA66 (see table 1). At higher CNT contents the onset crystallization temperature $T_{c,o}$ increases marginally, whereas the maximum crystallization temperature $T_{c,m}$ was found to be constant. It can be concluded that already low CNT contents show a nucleating effect in polyamide 66 composites. For a PA66 composite containing 2 wt.% NC7000 the same tendencies in the thermal behaviour were reported from Krause et al. [24], however the mixing conditions in this study were different. Thereby, an increase of 16 K (238°C up to 254°C) in the onset crystallization temperature $T_{c,o}$ and of 10 K (237°C up to 247°C) in the maximum

crystallization temperature $T_{c,m}$ were determined. An increase of the crystallization temperature from 233 °C to 243-245 °C nearly independent on the CNT content (1-10 wt.%) was also found by Caamaño et al. [21] and Baji et al. [22] which is consistent with the results of the present study. In another study, Qiu et al. [23] described for the incorporation of 1 wt.% MWCNTs into PA66 an increase of the crystallization temperature from 232 °C to 240 °C, 243 °C or 244 °C for the diamine-modified, acidified, or purified MWCNTs, respectively.

The melting behaviour of PA66 was not influenced by the incorporation of both types of nanotubes (Table 1). This finding is in agreement with the results of other authors [21, 22, 24].

The crystallinity α of the MWCNT 1 filled PA66 composites varies between 39 and 43% (see table 1). In comparison to the values of the pure PA66 (α = 40-41%), no clear dependency of the crystallinity on the nanotube content could be determined. In contrast to our results, in the literature [22-24] the nanotube incorporation is reported to result in an increase of crystallinity α. Qiu et al. [23] described an increase of the overall crystallinity from 28% to 33-34% with the MWCNT incorporation (1 wt.%) depending on the MWCNT functionalization. A raise of crystallinity from 33% to 36% after filling the polyamide with 1 wt.% MWCNT was also found by Baji et al. [22]. A change of crystallinity from 41% for pure PA66 to 46% for PA66 filled with 2 wt.% MWCNTs was reported from Krause et al. [24] (table 1).

Interestingly, for the crystallinity of the MWCNT 2/0.05 wt% PA66 composite a decrease of 4% compared to pure PA66 was determined. This finding can discuss in context with the state of CNT dispersion. The correlation between the electrical percolation threshold and the crystallinity described from Jeon et al. [26] for

polyethylene and polypropylene-ethylene copolymers with SWCNTs is unsuitable as an explanation for the differences, as the PA66 crystallinity is around 40% and hence in a region where the percolation threshold should be independent of crystallinity. In context with the finding of Villmow et al. [25] that the crystallinity was as higher as better the nanotube dispersion and thus the amount of CNT surface exposed to the matrix for initiating crystallization, it can assumed that the decrease of the crystallinity of PA66/MWCNT 2 is an indication of a worse CNT dispersion in comparison to the PA66/MWCNT 1 composite. The light microscopy images in [1] (Fig. 9d (MWCNT2) and 9e (MWCNT 1)) support this conclusion. The macrodispersion of the much shorter NC7000 in the PA 66 matrix was found to be significantly better than the one of MWCNT 1 (see Figure 3). For the PA66/NC7000 composites an increase in crystallinity of 5% was observed [24] (table 1). The better CNT dispersion and the higher crystallinity of PA66/NC7000 in comparison to the PA66/MWCNT 1 and 2 composites and the differentiation between the effects of MWCNT1 and MWCNT 2 correlate with the finding of Villmow et al.. The results of the thermal behavior hence indicate that the aerosol- synthesized MWCNTs act as nucleating agents; however, the degree of perfection of the crystallites is not significantly improved. It can be concluded that the very long MWCNTs hinder the crystal growth and show a worse macrodispersion in comparison to the shorter NC7000, however lead to much lower percolation thresholds.

4. Summary

A very low electrical percolation threshold of 0.04-0.05 wt.% was found for melt mixed PA66 composites containing multiwalled carbon nanotubes synthesized via aerosol-

catalytically vapour deposition technique. The incorporated nanotubes were very long and stretched in the as-grown state as well after melt processing. In the composites the nanotubes formed a conductive network already at a concentration of 0.04 wt.% caused by high length of MWCNTs and the good dispersion at the nano scale. Interestingly, the ultralow electrical percolation threshold is governed by the aspect ratio and the state of dispersion in nano scale rather than by the electrical conductivity of the nanotube powder and the CNT macrodispersion. For PA66/ Nanocyl^{TM} NC7000 samples prepared under comparable conditions [24] a higher electrical percolation threshold was found which can be assigned to the fact that these nanotubes are significantly shorter and more entangled as well before as after melt mixing.

The investigation of the thermal behaviour showed a significant nucleation effect of both MWCNTs and no significant change (MWCNT 1) or decrease (MWCNT 2) of the overall polyamide crystallinity. It was found that the composite crystallinity correlate with the state of CNT macrodispersion. The highest crystallinity was measured for the PA66/NC7000 composites which also showed the best CNT macrodispersion. The worst CNT macrodispersion was observed of the PA66/MWCNT 2 composite having the lowest crystallinity.

Acknowledgement

The authors thank the Bundesministerium für Bildung und Forschung (BMBF) for financial support within the project 03X3006. We thank Albrecht Leonhardt and Manfred Ritschel (Leibniz Institute for Solid State and Materials Research Dresden) for the synthesis of the MWCNTs using the aerosol method.

References

[1] Krause B, Ritschel M, Täschner C, Oswald S, Gruner W, Leonhardt A, Pötschke P. Comparison of nanotubes produced by fixed bed and aerosol-CVD methods and their electrical percolation behaviour in melt mixed polyamide 6.6 composites. Composites Science and Technology 2010;70(1):151-160.

[2] Krause B, Mende M, Pötschke P, Petzold G. Dispersability and particle size distribution of CNTs in an aqueous surfactant dispersion as a function of ultrasonic treatment time. Carbon 2010;48(10):2746-2754.

[3] Krause B, Boldt R, Pötschke P. A method for determination of length distributions of multiwalled carbon nanotubes before and after melt processing. Carbon 2011;49(4):1243-1247.

[4] Alig I, Pötschke P, Lellinger D, Skipa T, Pegel S, Kasaliwal GR, Villmow T. Establishment, morphology and properties of carbon nanotube networks in polymer melts. Polymer 2012;53(1):4-28.

[5] Stauffer D, Aharony A. Introduction in percolation theory. London: Taylor and Francis, 1994.

[6] Xu DH, Wang ZG, Douglas JF. Influence of Carbon Nanotube Aspect Ratio on Normal Stress Differences in Isotactic Polypropylene Nanocomposite Melts. Macromolecules 2008;41(3):815-825.

[7] Guo J, Liu Y, Prada-Silvy R, Tan Y, Azad S, Krause B, Pötschke P, Grady BP. Aspect ratio effects of multi-walled carbon nanotubes on electrical, mechanical, and thermal properties of polycarbonate/MWCNT composites. Journal of Polymer Science Part B: Polymer Physics 2014;52(1):73-83.

[8] Castillo FY, Socher R, Krause B, Headrick R, Grady BP, Prada-Silvy R, Pötschke P. Electrical, mechanical, and glass transition behavior of polycarbonate-based nanocomposites with different multi-walled carbon nanotubes. Polymer 2011;52(17):3835-3845.

[9] Li F, Lu Y, Liu L, Zhang L, Dai J, Ma J. Relations between carbon nanotubes' length and their composites' mechanical and functional performance. Polymer 2013;54(8):2158-2165.

[10] Ayatollahi MR, Shadlou S, Shokrieh MM, Chitsazzadeh M. Effect of multi-walled carbon nanotube aspect ratio on mechanical and electrical properties of epoxy-based nanocomposites. Polymer Testing 2011;30(5):548-556.

[11] Krause B, Mende M, Petzold G, Boldt R, Pötschke P. Characterization of dispersability of industrial nanotube materials and their length distribution before and after melt processing. In: Tasis D, ed. Carbon Nanotube-Polymer Composites, Cambridge, UK: Royal Society of Chemistry, 2013.

[12] Krause B, Villmow T, Boldt R, Mende M, Petzold G, Pötschke P. Influence of dry grinding in a ball mill on the length of multiwalled carbon nanotubes and their dispersion and percolation behaviour in melt mixed polycarbonate composites. Composites Science and Technology 2011;71(8):1145-1153.

[13] Pötschke P, Villmow T, Krause B. Melt mixed PCL/MWCNT composites prepared at different rotation speeds: Characterization of rheological, thermal, and electrical properties, molecular weight, MWCNT macrodispersion, and MWCNT length distribution. Polymer 2013;54(12):3071-3078.

[14] Socher R, Krause B, Müller MT, Boldt R, Pötschke P. The influence of matrix viscosity on MWCNT dispersion and electrical properties in different thermoplastic nanocomposites. Polymer 2012;53(2):495-504.
[15] Park KS, Youn JR. Dispersion and aspect ratio of carbon nanotubes in aqueous suspension and their relationship with electrical resistivity of carbon nanotube filled polymer composites. Carbon 2012;50(6):2322-2330.
[16] Park HJ, Park M, Chang JY, Lee H. The effect of pre-treatment methods on morphology and size distribution of multi-walled carbon nanotubes. Nanotechnology 2008;19(33):335702.
[17] Lu KL, Lago RM, Chen YK, Green MLH, Harris PJF, Tsang SC. Mechanical damage of carbon nanotubes by ultrasound. Carbon 1996;34(6):814-816.
[18] Chen SJ, Zou B, Collins F, Zhao XL, Majumber M, Duan WH. Predicting the influence of ultrasonication energy on the reinforcing efficiency of carbon nanotubes. Carbon 2014;77:1-10.
[19] Wu Z, Mitra S. Length reduction of multi-walled carbon nanotubes via high energy ultrasonication and its effect on their dispersibility. Journal of Nanoparticle Research 2014;16(8):2563 (2561-2567).
[20] Krause B, Petzold G, Pegel S, Pötschke P. Correlation of carbon nanotube dispersability in aqueous surfactant solutions and polymers. Carbon 2009;47(3):602-612.
[21] Caamano C, Grady B, Resasco DE. Influence of nanotube characteristics on electrical and thermal properties of MWCNT/polyamide 6,6 composites prepared by melt mixing. Carbon 2012;50(10):3694-3707.
[22] Baji A, Mai Y-W, Wong S-C, Abtahi M, Du X. Mechanical behavior of self-assembled carbon nanotube reinforced nylon 6,6 fibers. Composites Science and Technology 2010;70(9):1401-1409.
[23] Qiu L, Yang Y, Xu L, Liu X. Influence of surface modification of carbon nanotube on microstructures and properties of polyamide 66/multiwalled carbon nanotube composites. Polymer Composites 2013;34(5):656-664.
[24] Krause B, Pötschke P, Häußler L. Influence of small scale melt mixing conditions on electrical resistivity of carbon nanotube-polyamide composites. Composites Science and Technology 2009;69(10):1505-1515.
[25] Villmow T, Pötschke P, Pegel S, Häussler L, Kretzschmar B. Influence of twin-screw extrusion conditions on the dispersion of multi-walled carbon nanotubes in a poly(lactic acid) matrix. Polymer 2008;49(16):3500-3509.
[26] Jeon K, Warnock S, Ruiz-Orta C, Kismarahardja A, Brooks J, Alamo RG. Role of matrix crystallinity in carbon nanotube dispersion and electrical conductivity of iPP-based nanocomposites. Journal of Polymer Science Part B: Polymer Physics 2010;48(19):2084-2096.
[27] Bauhofer W, Kovacs JZ. A review and analysis of electrical percolation in carbon nanotube polymer composites. Composites Science and Technology 2009;69(10):1486-1498.
[28] Loos J, Alexeev A, Grossiord N, Koning CE, Regev O. Visualization of single-wall carbon nanotube (SWNT) networks in conductive polystyrene nanocomposites by charge contrast imaging. Ultramicroscopy 2005;104(2):160-167.
[29] Menczel JD, Jaffe M, Bessey WE. Films. In: Turi EA, ed. Thermal characterization of polymeric materials, San Diego: Academic Press Inc., 1997.

[30] Kasaliwal GR, Pegel S, Göldel A, Pötschke P, Heinrich G. Analysis of agglomerate dispersion mechanisms of multiwalled carbon nanotubes during melt mixing in polycarbonate. Polymer 2010;51(12):2708-2720.
[31] Kasaliwal GR, Göldel A, Pötschke P, Heinrich G. Influences of polymer matrix melt viscosity and molecular weight on MWCNT agglomerate dispersion. Polymer 2011;52(4):1027-1036.
[32] Zhuravlev E, Wurm A, Pötschke P, Androsch R, Schmelzer JWP, Schick C. Kinetics of nucleation and crystallization of poly(ε-caprolactone) – Multiwalled carbon nanotube composites. European Polymer Journal 2014;52:1-11.
[33] Trujillo M, Arnal ML, Müller AJ, Mujica MA, Urbina de Navarro C, Ruelle B, Dubois P. Supernucleation and crystallization regime change provoked by MWNT addition to poly(ε-caprolactone). Polymer 2012;53(3):832-841.

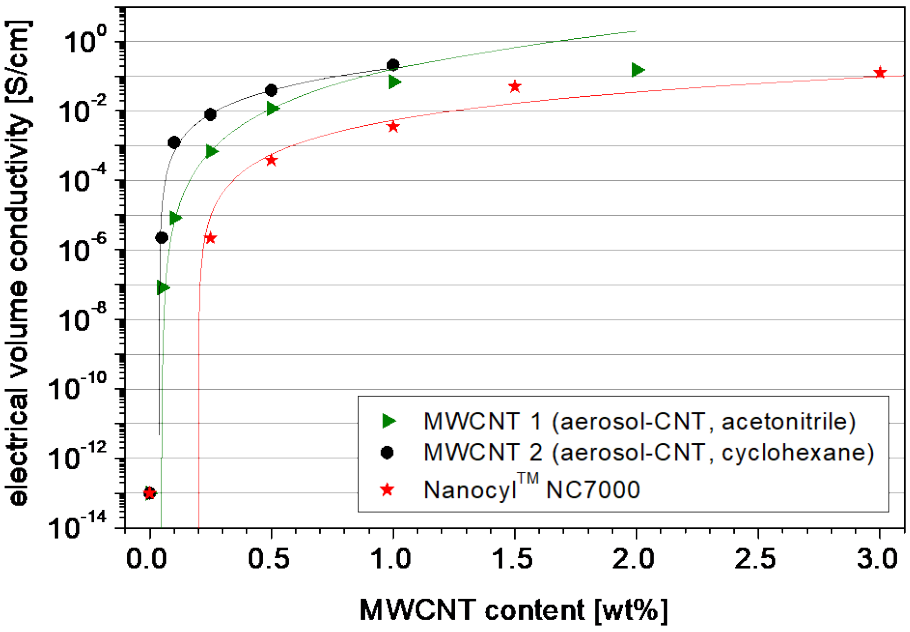

Figure 1 - Electrical volume conductivity of PA66 composites containing different CNTs, adapted from Refs. [1, 20]

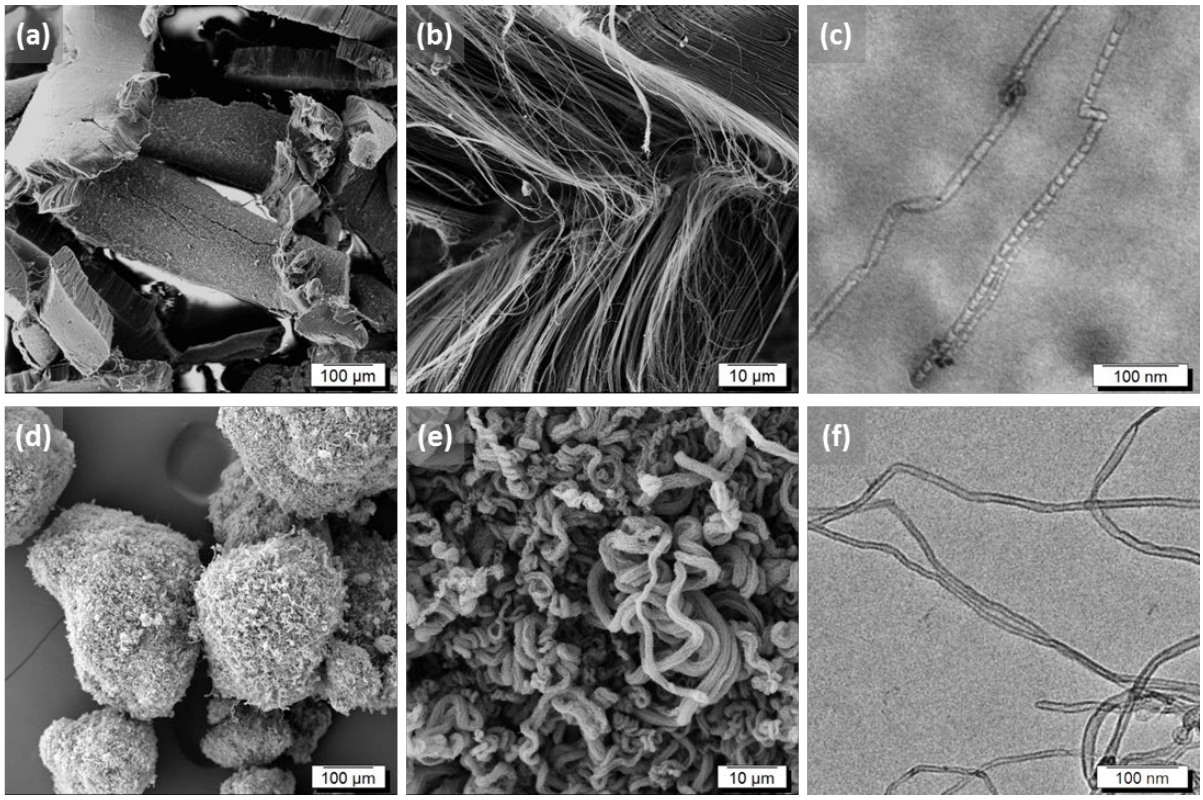

Figure 2 – Morphology of MWCNT1 (SEM images: a, b; TEM image: c) and NC7000 (SEM images: d, e; TEM image: f)

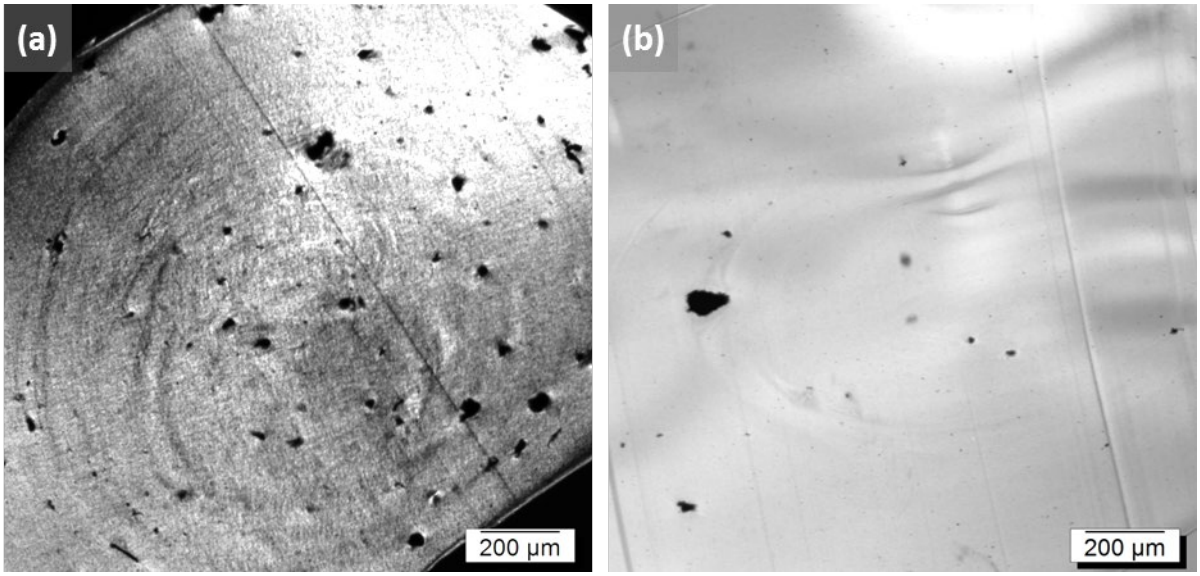

Figure 3 - LM images of polyamide 6.6 filled (a) with 0.05 wt.% MWCNTs 1 and (b) 0.05 wt.% NC7000

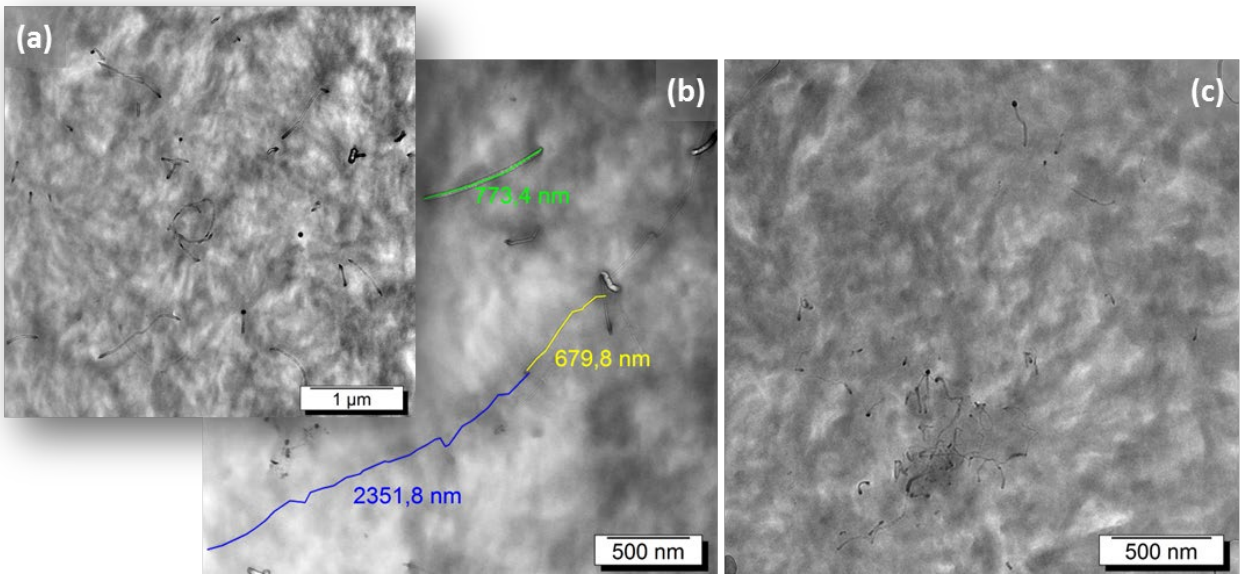

Figure 4 - TEM images of PA66 filled with (a, b) 0.05 wt.% MWCNTs 1 and (c) 0.05 wt.% NC7000

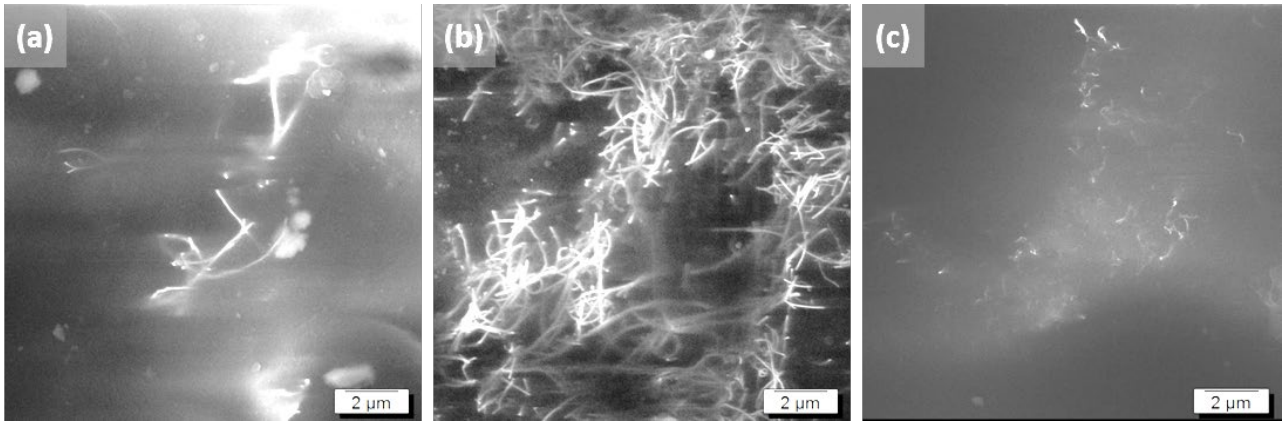

Figure 5 - SEM images (CCI mode) of polyamide 6.6 filled with (a) 0.05 wt.% MWCNTs 1, (b) 1 wt.% MWCNTs 1, (c) 1 wt.% NC7000.

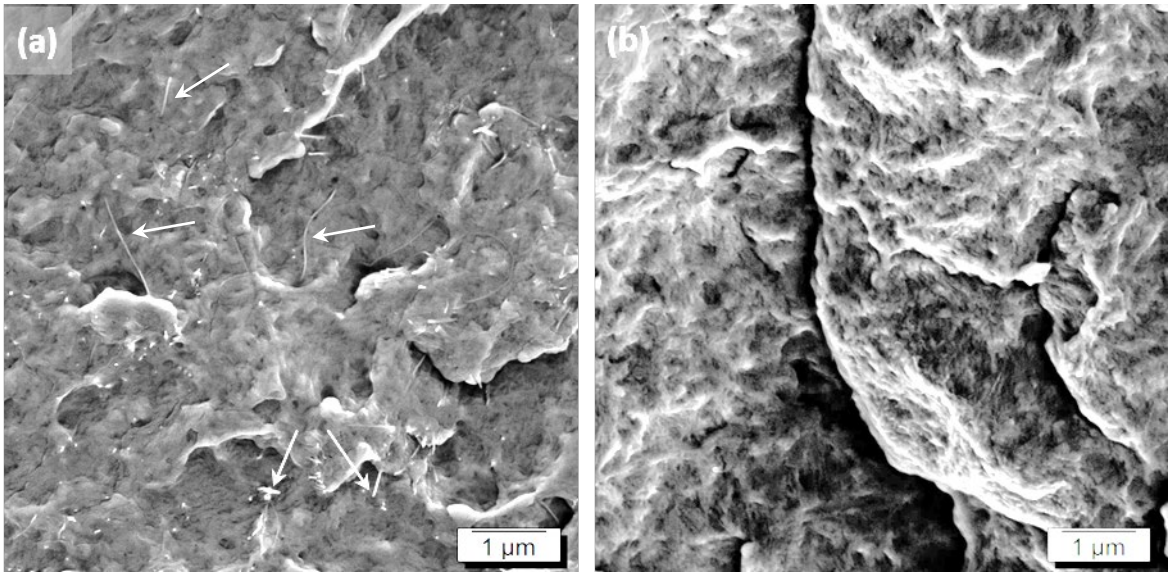

Figure 6 - SEM images of the cryofractured surfaces of polyamide 6.6 filled with (a) 0.05 wt.% MWCNTs 1 and (b) NC7000.

Tables

Table 1 - DSC data of PA66 and PA66 composites filled with different MWCNTs

	T_m [°C]	$T_{c,o}$ [°C]	$T_{c,m}$ [°C]	ΔH [J/g]	α [%]
PA66	262	238	233	76	40
PA66 melt processed*	263	238	237	78	41
MWCNT 1, bamboo-like					
PA66 + 0.05 wt.% MWCNT 1	263	249	244	77	41
PA66 + 0.10 wt.% MWCNT 1	263	249	244	75	39
PA66 + 0.25 wt.% MWCNT 1	263	250	245	82	43
PA66 + 0.50 wt.% MWCNT 1	262	251	245	81	43
PA66 + 1.00 wt.% MWCNT 1	262	252	245	78	41
MWCNT 2, tubular					
PA66 + 0.05 wt.% MWCNT 2	263	249	244	71	37
NC7000					
PA66 + 2.00 wt.% NC7000 [24]	261	254	247	88	46

* melt processing conditions: 280°C, 5 min, 50 rpm